

UNSTEADY RADIATIVE-CONDUCTIVE HEAT TRANSFER IN A POROUS,  
PERMEABLE LAYER OF A SEMITRANSSPARENT MEDIUM

A. L. Burka and V. V. Dudkin

UDC 536.33

We consider the unsteady problem of radiative-conductive heat transfer in a plane, porous-permeable layer of a gray medium. In the one-dimensional approximation, the boundary-value problem has the form [1]:

$$(1 - m)\rho c \frac{\partial T}{\partial t} + m\rho_f c_f v \frac{\partial T}{\partial x} = \frac{\partial}{\partial x} \left( \lambda \frac{\partial T}{\partial x} \right) - \frac{\partial q}{\partial x}, \quad t > 0; \quad (1)$$

$$\lambda \frac{\partial T}{\partial x} = (\alpha_1 + m\rho_f c_f v)(T - T_1) + \varepsilon_1 \sigma (T^4 - T_1^4), \quad x = x_0; \quad (2)$$

$$\lambda \frac{\partial T}{\partial x} = (\alpha_2 + m\rho_f c_f v)(T_2 - T) + \varepsilon_2 \sigma (T_2^4 - T^4), \quad x = x_1; \quad (3)$$

$$T(x, 0) = T_0(x), \quad x \in [x_0, x_1], \quad (4)$$

where

$$\begin{aligned} \frac{\partial q}{\partial x} = & 2\kappa\sigma n^2 \left\{ 2T^4(x, t) - T^4(x_0, t) K_2(\kappa x) - T^4(x_1, t) K_2(\kappa(x_1 - x)) - \right. \\ & \left. - \kappa \int_{x_0}^{x_1} T^4(z, t) K_1(\kappa|x - z|) dz \right\}; \\ K_j(x) = & \int_0^1 z^{j-2} \exp\left(-\frac{x}{z}\right) dz; \end{aligned}$$

$m$  is the material porosity;  $\rho$ ,  $\rho_f$ ,  $c$ ,  $c_f$  are the density and heat capacity of the material and the coolant;  $\lambda$  is the thermal conductivity of the material taking porosity into account;  $\alpha_1$ ,  $\alpha_2$ ,  $\varepsilon_1$ ,  $\varepsilon_2$  are the coefficients of surface heat release and the degree of blackness for the heated and cooled sides, respectively;  $v$  is the transfer rate of coolant;  $n$  is the index of refraction; and  $\kappa$  the absorption coefficient of the material.

Assuming that the mass outflux of coolant  $g = \rho_f v$  is constant, and that the material-temperature dependence of  $c_f$  can be neglected, we make the boundary-value problem (1)-(4) dimensionless in the following fashion:

$$\begin{aligned} \theta = T/T_*, \quad \omega_1 = T_1/T_*, \quad \omega_2 = T_2/T_*, \quad \theta_0 = T_0/T_*, \quad \bar{c} = c/c_*, \\ \bar{\lambda} = \lambda/\lambda_*, \quad \tau = t/t_*, \quad x = L\xi + x_0, \quad L = x_1 - x_0, \quad \xi \in [0, 1]. \end{aligned}$$

Here,  $T_*$  and  $t_*$  are characteristic temperature and time;  $c_*$  and  $\lambda_*$  the characteristic heat capacity and thermal conductivity of the material.

Introducing the notation

$$\begin{aligned} \omega = (1 - m)\rho c_* L^2 / (t_* \lambda_*), \quad \text{Pe} = m c_f g L / \lambda_*, \\ N_{U_i} = \alpha_i L / \lambda_*, \quad L_0 = L \kappa, \quad S_k = \sigma T_*^3 L / \lambda_*, \quad i = 1, 2, \end{aligned}$$

and omitting the bar over the dimensionless variables  $\bar{c}$ ,  $\bar{\lambda}$ , we obtain a statement of boundary-value problem (1)-(4):

$$\omega c \frac{\partial \theta}{\partial \tau} + \text{Pe} \frac{\partial \theta}{\partial \xi} = \frac{\partial}{\partial \xi} \left( \lambda \frac{\partial \theta}{\partial \xi} \right) - S_k \frac{\partial \Phi}{\partial \xi}, \quad \tau > 0, \quad \xi \in [0, 1]; \quad (5)$$

$$\lambda \frac{\partial \theta}{\partial \xi} = (N_{U_1} + \text{Pe})(\theta - \omega_1) + \varepsilon_1 S_k (\theta^4 - \omega_1), \quad \xi = 0; \quad (6)$$

$$\lambda \frac{\partial \theta}{\partial \xi} = -(N_{U_1} + \text{Pe})(\theta - \omega_2) + \varepsilon_2 S_k (\omega_2^4 - \theta^4), \quad \xi = 1; \quad (7)$$

$$\theta(\xi, 0) = \theta_0(\xi). \quad (8)$$

In this case

$$\frac{\partial \Phi}{\partial \xi} = 2L_0 n^2 \left\{ 2\theta^4(\xi, \tau) - K_2(L_0 \xi + x_0) \theta^4(0, \tau) - K_2(L_0(1 - \xi)) \theta^4(1, \tau) - L_0 \int_0^1 \theta^4(z, \tau) K_1(L_0 |\xi - z|) dz \right\}.$$

We consider a procedure for numerical solution of boundary-value problem (5)-(8) using the collocation finite element method [2]. We break up the one-dimensional computational region  $\xi \in [0, 1]$  into  $\ell$  three-noded finite elements. Then  $\ell_1 = 2\ell + 1$  is the number of nodes in the computational region.

Dividing the computational region into  $\ell_1 - 1$  subintervals and setting

$$z = \Delta z(\tau + i - 1), \quad \Delta z = 1/(\ell_1 - 1), \quad i = 1, 2, \dots, \ell_1 - 1,$$

we have

$$K_1(\xi) = \Delta z \sum_{i=1}^{\ell_1} \int_0^1 \exp\left(-\frac{\xi}{z}\right) \frac{d\tau}{z}, \quad K_2(\xi) = \Delta z \sum_{i=1}^{\ell_1} \int_0^1 \exp\left(-\frac{\xi}{z}\right) d\tau.$$

Finally, introducing the substitution of variables  $J = 2\tau - 1$ ,  $J \in [-1, 1]$ , we obtain an approximation for the exponential integrals

$$K_1(\xi) = \frac{\Delta z}{2} \sum_{i=1}^{\ell_1} \sum_{j=1}^r \gamma_j \exp\left(-\frac{\xi}{z_j}\right) \Big|_{z_j},$$

$$K_2(\xi) = \frac{\Delta z}{2} \sum_{i=1}^{\ell_1} \sum_{j=1}^r \gamma_j \exp\left(-\frac{\xi}{z_j}\right).$$

Here  $\gamma_j$  are weights;  $z_j$  the Gaussian quadrature nodes;  $z_j = \Delta z(i - 1 + (J_j + 1)/2)$ ;  $r$  is the order of the Gaussian quadrature formula. To approximate the integral term in (6)  $\int_0^1 \theta^4(\eta, \tau) \times d\tau$ , we use a finite element representation, setting

$$\theta(\eta, \tau) = \theta_\mu(\tau) N^\mu(\eta), \quad \mu = 1, 2, 3$$

in the finite element. (There is implied summation over the index  $\mu$ .  $\theta_\mu$  are the nodal values of  $\theta$ ,  $N^\mu$  are the finite element basis functions.)

Then

$$\theta(\eta, \tau) = \sum_{\mu=1}^3 \{\theta_\mu(\tau) N^\mu(\eta)\}^4.$$

Introducing the notation

$$I_\mu(\xi) = \delta \int_0^1 (N^1)^\alpha (N^2)^\beta (N^3)^\gamma K_1(L_0 |\xi - \eta|) d\eta,$$

where the indices  $\alpha, \beta, \gamma, \delta$ , and  $\mu$  are defined in Table 1, we obtain

$$I(\xi) = \sum_{\mu=1}^{\ell_1} I_\mu(\xi) \theta_1^\alpha \theta_2^\beta \theta_3^\gamma.$$

We apply the finite element method of collocation in  $\xi$ , and an implicit finite difference scheme of first order in  $\tau$  to Eqs. (5)-(8). As a result, at the nodes of the computational region we have a system of  $\ell_1$  nonlinear algebraic equations:

$$\left( \Lambda_v \frac{\partial^2 N^\mu}{\partial \xi^2} + \frac{\partial \Lambda_v}{\partial \xi} \frac{\partial N^\mu}{\partial \xi} - \text{Pe} \frac{\partial N^\mu}{\partial \xi} + \frac{\omega}{\Delta \tau} c_v \delta_v^\mu \right) \theta_\mu - S_k \frac{\partial \Phi_v}{\partial \xi} = \frac{\omega}{\Delta \tau} c_v \theta_{0v}; \quad (9)$$

TABLE 1

$\alpha$	$\beta$	$\gamma$	$\delta$	$\mu$	$\alpha$	$\beta$	$\gamma$	$\delta$	$\mu$
4	0	0	1	1	1	1	2	12	9
0	4	0	1	2	1	1	0	4	10
0	0	4	1	3	3	3	0	4	11
2	2	0	6	4	1	0	1	4	12
2	0	2	6	5	3	0	3	4	13
2	2	2	6	6	0	3	1	4	14
0	1	1	12	7	0	1	3	4	15
2	2	1	12	8					

TABLE 2

$T$	$c$	$\lambda$	$T$	$c$	$\lambda$
10	0,80	0,30	2000	2,10	0,62
300	0,88	0,35	2500	2,16	0,70
500	1,22	0,40	3005	2,21	0,74
1500	1,80	0,50			

$$\begin{aligned} & \left( \Lambda_1 \frac{\partial N^\mu}{\partial \xi} - (N_{U_1} + Pe) \delta_1^\mu \right) \theta_\mu - \varepsilon_1 S_k \theta_1^4 = \\ & = -\omega_1 (N_{U_1} + Pe + \varepsilon_1 S_k \omega_1^3), \quad \xi = 0; \end{aligned} \quad (10)$$

$$\begin{aligned} & \left( \Lambda_1 \frac{\partial N^\mu}{\partial \xi} + (N_{U_2} + Pe) \delta_1^\mu \right) \theta_\mu + \varepsilon_2 S_k \theta_1^4 = \\ & = -\omega_2 (N_{U_2} + Pe + \varepsilon_2 S_k \omega_2^3), \quad \xi = 1; \end{aligned} \quad (11)$$

$$\begin{aligned} \frac{\partial \Phi_\nu}{\partial \xi} &= 2L_0 n^2 \{ 2\theta_\nu^4 - K_2 (L_0 \xi + x_0) \theta_1^4 - K_2 (L_0 (1 - \xi)) \theta_1^4 - L_0 I(\xi) \}, \\ & \xi \in [0, 1], \quad \nu = 2, \dots, l_1 - 1. \end{aligned}$$

Here  $c_\nu$ ,  $\lambda_\nu$  are the nodal values of  $c$  and  $\lambda$ ;  $\delta_\nu^\mu$  is the Kronecker delta symbol.

Applying Newton's method [3] to system (9)-(11), we have  $\theta_\nu = \bar{\theta}_\nu + \Delta\theta_\nu$ . Here  $\bar{\theta}_\nu$  is the starting approximation (in the first time step, the initial data are used for this value), and  $\Delta\theta_\nu$  is a small correction term. System (9)-(11) reduces to a system of linear algebraic equations of the form

$$Q^{\nu\mu} \Delta\theta_\mu = R^\nu. \quad (12)$$

Explicit expressions for the coefficients  $Q$ ,  $R$  are not given, due to the unwieldiness of these expressions. At each time step, the solution to system (12) is sought until the condition  $|\Delta\theta_\nu| < \varepsilon$  is satisfied for all  $\nu$  ( $\varepsilon$  is a small quantity on the order of  $10^{-5}$ - $10^{-6}$ ).

This algorithm was implemented in FORTRAN-77 on an IBM PC/AT286. The average computational time on a mesh of 10 finite elements (21 nodes) is 7-10 min.

Below we give the results of calculations done using the following thermophysical and optical parameters:  $\Delta\tau = 6 \cdot 10^{-4}$ ,  $N_{U_1} = 1.22$ ,  $N_{U_2} = 0.12$ ,  $S_k = 18.84$ ,  $\omega_1 = 0.9$ ,  $\omega_2 = 0.1$ ,  $\theta_0 = 0.5$ ,  $Pe = 9.92$ ,  $T_x = 3000$  K,  $L = 0.03$  m,  $n = 1.5$ ,  $\varepsilon_1 = 0.85$ ,  $\varepsilon_2 = 0.35$ .

The results of solving the system of equations (12) reflect the dynamics of the heating of a plane, semitransparent body whose surface is exposed to radiative-convective heating. These results are shown in Figs. 1-3.

Figure 1 shows the dimensionless temperature  $\theta$  as a function of the dimensionless coordinates  $\xi$  for an initial dimensionless temperature of  $\theta_0 = 0.5$ , with constant heat capacity and thermal conductivity. In this figure, the numbers above the curve correspond to the dimensionless time. Figure 2 illustrates the temperature distribution for the same parameters, but with  $\theta_0 = 0.1$ . Figure 3 shows the temperature field for an initial temperature of  $\theta_0 = 0.5$  and with variable  $c(\theta)$ ,  $\lambda(\theta)$ . The temperature dependences of the latter are given in Table 2.

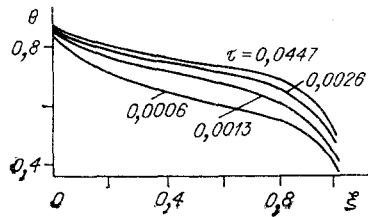


Fig. 1

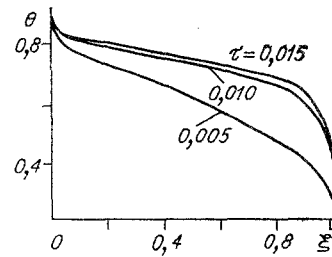


Fig. 2

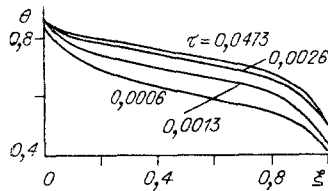


Fig. 3

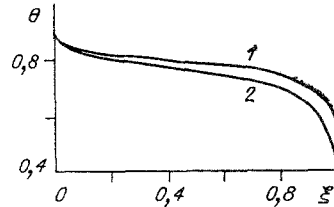


Fig. 4

The parametric dependence of the temperature distribution on  $Pe = 2, 10$  (curves 1, 2) is shown in Fig. 4 for dimensionless time  $\tau = 0.01$  and  $\theta_0 = 0.5$ . It is evident that with increasing separation of the hot and cold surfaces, the temperature curves increasingly differ from one another, both quantitatively and qualitatively. This is explained by the fact that because the velocity of the injected gas increases with increasing distance from the hot wall, the hot gas is not able to release heat to the solid skeleton. The temperature fields shown in the figures for various thermophysical and optical properties quite rapidly approach a steady state.

We compared calculations in which the dimensionless values  $c, \lambda$  were constant in time with those in which these values depended on  $\theta(\xi, \tau)$ . In the second case, these values were approximated by those given in Table 2. It is clear from an analysis of the computational results that taking the dependence of  $c$  and  $\lambda$  on  $\theta$  into account drags out the time it takes to approach a steady state and insignificantly influences the quantitative indicators.

#### LITERATURE CITED

1. A. L. Burka and E. P. Chirkashenko, "Radiative-conductive heat exchange in a porous rigid body," *Izv. Akad. Nauk SSSR, Sib. Otd. Ser. Tekh. Nauk*, No. 3 (1986).
2. V. V. Dudkin and A. A. Oksogoev, "Finite element method with collocation in the study of coupled problems in aeroelasticity of soft shells," Abstracts for papers given at the 2nd All-Union Conference: Contemporary Problems in Mechanical Engineering and the Strength of Flying Devices, Moscow (1986).
3. L. V. Kantorovich, "On Newton's method," *Tr. Mat. Inst. Akad. Nauk SSSR*, 28 (1949).